Article:

Moyer, A.N., Sutherland, D.A., Nienow, P.W. et al. (1 more author) (2019) Seasonal variations in iceberg freshwater flux in Sermilik Fjord, southeast Greenland from Sentinel-2 imagery. Geophysical Research Letters, 46 (15). pp. 8903-8912. ISSN 0094-8276

https://doi.org/10.1029/2019gl082309

Seasonal variations in iceberg freshwater flux in Sermilik Fjord, southeast Greenland from Sentinel-2 imagery

A. N. Moyer[1], D. A. Sutherland[2], P. W. Nienow[1], and A. J. Sole[3]

[1]School of Geosciences, University of Edinburgh, Edinburgh, UK. [2]Department of Earth Sciences, University of Oregon, Eugene, OR. [3]Department of Geography, University of Sheffield, Sheffield, UK.

Corresponding author: Alexis Moyer (a.moyer@ed.ac.uk)

Key Points:

- Freshwater fluxes from iceberg melt in Sermilik Fjord have a seasonal signal, peaking across August and September in 2017 and 2018.
- Fluxes decrease with distance down-fjord from Helheim Glacier, with ~86-91% of iceberg volume lost before reaching the fjord mouth.
- We present a simple and effective tool for monitoring iceberg freshwater fluxes across a range of Greenlandic fjords.

Abstract

Iceberg discharge is estimated to account for up to 50% of the freshwater flux delivered to glacial fjords. The amount, timing and location of iceberg melting impacts fjord-water circulation and heat budget, with implications for glacier dynamics, nutrient cycling and fjord productivity. We use Sentinel-2 imagery to examine seasonal variations in freshwater flux from open-water icebergs in Sermilik Fjord, Greenland during summer and fall of 2017-2018. Using iceberg velocities derived from visual-tracking and changes in total iceberg volume with distance down-fjord from Helheim Glacier, we estimate maximum average 2-month full-fjord iceberg-derived freshwater fluxes of ~1060±615, 1270±735, 1200±700, 3410±1975, and 1150±670 $m^3 s^{-1}$ for May-June, June-July, July-August, August-September and September-November, respectively. Fluxes decrease with distance down-fjord and on average, 86-91% of iceberg volume is lost before reaching the fjord mouth. This method provides a simple, invaluable tool for monitoring seasonal and inter-annual iceberg freshwater fluxes across a range of Greenlandic fjords.

Plain Language Summary

Recent studies have shown that the freshwater produced via the melting of icebergs can dominate the freshwater budget in glacial fjords surrounding the Greenland Ice Sheet, which has important implications for fjord circulation and heat budget, nutrient availability and primary productivity. Here, we use satellite imagery to estimate both iceberg velocity and the seasonal changes in iceberg volume in Sermilik Fjord in southeast Greenland in 2017-2018, from which meltwater fluxes are derived. Iceberg meltwater fluxes are highest in the late summer and fall, when fjord water temperatures are warmer than in the spring and early summer, and when more icebergs have been calved into the fjord. Throughout the year, the volume of freshwater generated from the melting of icebergs is greater than the freshwater entering the fjord at the base of the glacier and sourced from melting at the ice sheet surface. As such, the melting of icebergs provides a significant volume of freshwater to the fjord system, with important implications for fjord-scale circulation and heat budget, nutrient cycling and primary productivity. The methodology presented here is effective, simple and inexpensive, and can be applied to a variety of glacial fjord systems, particularly those that are remote and inaccessible.

1 Introduction

Recent studies have shown that meltwater fluxes from icebergs can dominate the freshwater budget in glacial fjords surrounding the Greenland Ice Sheet (Enderlin et al., 2016; Moon et al., 2017). The amount, timing and location of meltwater delivered from icebergs to a fjord system has important glaciological and ecological implications. The energy lost through the melting of icebergs and the input of cold freshwater at various depths in the water column alters the amount of heat reaching tidewater glaciers (Enderlin et al., 2016), with implications for terminus submarine melting. This is of particular importance, as submarine melting of glacier termini has been proposed as a trigger for glacier calving, retreat and acceleration (O*'Leary and* Christoffersen, 2013; Luckman et al., 2015). The input of freshwater at various fjord locations and depths also alters fjord salinity gradients, impacting not only buoyancy-driven circulation important to submarine melting, but also nutrient budgets and associated primary productivity and thus fishery stocks crucial for local economies (e.g., Rose, 2005; Smith et al., 2013; Meire et al., 2017).

Previous studies have used numerical iceberg models (e.g., Mugford and Dowdeswell, 2010; Moon et al., 2017) or remote sensing methods (e.g., Enderlin and Hamilton, 2014; Enderlin et al., 2016) to estimate iceberg melt rates and freshwater fluxes into glacial fjords. Moon et al. (2017) modeled iceberg melt using oceanographic and reanalysis data and modeled buoyant plume velocities to account for iceberg melting above, below and at the waterline. While providing a valuable methodology, modelling iceberg meltwater flux is very complex, relying heavily on sparse field data (including ocean temperature and salinity, water velocity, air temperature and wind speed) and poorly constrained model parameterizations. Enderlin and Hamilton (2014) and Enderlin et al. (2016) used changes in iceberg freeboard derived from high-resolution digital elevation models to estimate iceberg volume loss, from which area-averaged iceberg melt rates and fluxes were derived. Both of these methodologies are user-intensive (i.e., hand-digitizing hundreds of icebergs), data-heavy, expensive (requiring commercial satellite data and/or field data collection costs) and time-consuming. In addition, both methods assume standard iceberg underwater shapes, which significantly affect estimates of the submerged surface area and thus derived iceberg melt and freshwater fluxes.

Here, we use freely available Sentinel-2 satellite imagery from summer (June - September) and fall (November) 2017-2018 to estimate iceberg velocity and changes in iceberg volume with distance down-fjord from Helheim Glacier (HG) in Sermilik Fjord, southeast Greenland. From these data we generate seasonal, spatial estimates of iceberg freshwater flux into Sermilik Fjord. Our methodology can be transferred easily to other glacial fjords, thereby providing a valuable tool for generating widespread iceberg freshwater flux estimates.

2 Physical Setting

We use Sermilik Fjord in southeast Greenland as our study site (Figure 1a), as a range of oceanographic and glaciological measurements are available (e.g., Straneo et al., 2010; 2011; Sutherland et al., 2014a,b; Kehrl et al., 2017), as well as previous estimates of iceberg freshwater flux (e.g., Enderlin et al., 2016; Moon et al., 2017). At the head of the fjord are three large tidewater glaciers: Helheim, Fenris, and Midgård. Of these, Helheim is the most prolific iceberg producer, ~25 Gt a^{-1} (Enderlin et al., 2014), reaching speeds up to 11 km a^{-1} near the terminus (Kehrl et al., 2017). After exiting the ice mélange, which extends ~20 km east from the terminus, icebergs travel south for ~80 km before reaching the fjord mouth and the Irminger Sea. GPS-tracked icebergs from September 2012 and August 2013 show movement of ice within the fjord (see Figure 4c in Sutherland et al., 2014a), and while there is some inner-fjord iceberg recirculation, there is an overall net down-fjord movement of icebergs over time. Mooring data from the fjord in summer show a fresh, cool Polar Water surface layer (0 – 0.5 ºC) to depths between ~100-200 m underlain by a layer of salty, warm Atlantic Water (up to 5.2 ºC) (Sutherland et al., 2014b; Jackson et al., 2014).

3 Methodology

3.1 Estimating iceberg surface area and volume

To derive estimates of iceberg surface area, we use thirteen Sentinel-2 images acquired between June and November 2017-2018 (Table S1). Images were selected to minimize cloud and sea ice cover, which excluded all images prior to June and many fall images. The mean area of fjord analyzed per scene is ~649 km^2, with a smaller area (469 km^2) analyzed on 4 August 2017 and 18 June 2018 due to increased sea ice cover in the upper fjord. The near-infrared band (band

8, 10 m pixel size) of each image was converted to Top of Atmosphere (TOA) reflectance by dividing each pixel's digital number by the quantification value from each image's metadata (Gatti and Bertolini, 2015). A threshold was then applied to separate ice pixels from those containing water, using a value of 0.13 for summer images. This threshold was selected by testing a range of thresholds for each image, from 0.12 to 0.28, with 0.13 resulting in the best visual separation of ice and water pixels (see supporting information). Due to lower lighting conditions, we used a threshold value of 0.30 for the fall. Pixels with reflectance greater than or equal to these thresholds were automatically classified as ice and connected to adjacent ice pixels to form iceberg polygons (Figure 1b). Polygons were visually inspected, and erroneously coalesced icebergs were manually separated. Surface area was calculated for each iceberg polygon and summed per section of the fjord (white boxes in Figure 1a).

Iceberg volume was estimated by applying a known surface area-to-volume relationship, developed for Sermilik Fjord by Sulak et al. (2017). In their study, 712 icebergs were hand-delineated from Worldview digital elevation models of Sermilik Fjord between 2011-2014, from which they estimated above waterline volume and extrapolated below waterline volume, assuming the icebergs were floating in hydrostatic equilibrium. A general power law was fitted between planar iceberg surface area (A) and volume (V) (Sulak et al., 2017):

$$V = 6.0A^{1.3} \ (1).$$

We assume this relationship between iceberg surface area and volume holds true for other years in Sermilik Fjord, as we do not expect significant changes in calved ice properties or fjord water density. As noted in Sulak et al. (2017), the area exponent varies with iceberg shape, ranging from 1.0 to 1.5 for tabular and spherical/cubic icebergs, respectively. Following Sulak et al. (2017), and as there is a mix of iceberg shapes in Sermilik Fjord, a value of 1.3 was used. We recognize the uncertainty in the calculated power law constant and exponent, and we account for this in our estimation of iceberg freshwater flux uncertainty. In addition, as the unequal areas of each fjord section could lead to false trends in surface area with distance down-fjord, we normalized summed iceberg volumes by dividing by the total area of each fjord section.

3.2 Estimating iceberg velocity and freshwater flux

Iceberg velocity was estimated by visually-tracking six distinctly shaped icebergs throughout 16 Sentinel-2 images between June and September 2017; fourteen icebergs were tracked in 2018. The straight-line distance moved by the center of each iceberg between successive images was measured, and velocity was estimated as this distance divided by the time between images (Figure 1c). As icebergs do not move linearly, our estimates of distance and velocity are considered minimum values.

Following Sutherland et al. (2014a), we assume that mean iceberg movement is down-fjord, and that icebergs lose volume with movement due to melting. We estimate the freshwater flux from icebergs by imposing conservation of mass as the icebergs move down-fjord. Let $V(x,t)$ be the volume of icebergs at distance x from the glacier and time t. Conservation of mass may be stated as:

$$\frac{\partial V}{\partial t} + \frac{\partial}{\partial x}(Vu) + FW_{flux} = 0 \ (2)$$

where u is iceberg velocity. Under our method, which involves fitting a linear trend of iceberg volume along-fjord, the volume of icebergs at a given point, $\frac{\partial V}{\partial t}$, does not vary significantly in time (supporting information) and so is here set to 0. We furthermore assume a constant along-fjord iceberg velocity (see below), so that the freshwater flux from melting icebergs is written as:

$$FW_{flux} = -u\frac{\partial V}{\partial x} \quad (3)$$

Our 2017 freshwater flux estimates are 2-month average meltwater fluxes for the two months prior to the date of each Sentinel-2 scene, as it takes icebergs ~two months to travel the length of the fjord (as estimated based on mean iceberg velocity). For example, the freshwater fluxes derived from the image acquired on 13 September are average fluxes from mid-July to mid-September, as ice near the mouth of the fjord on 13 September would have been located near the head of the fjord in mid-July. Our 2018 estimates are only 1-month averages, as mean iceberg speed is faster. Throughout this paper, freshwater fluxes are temporally identified by the satellite image acquisition month.

Our analysis excludes all areas of the fjord covered by ice mélange, limiting our analysis to areas 37 km or greater from the HG terminus. In addition, we exclude both embayments found on the western side of the fjord (Figure 1a), as icebergs can become stuck here, and thus do not follow the assumed down-fjord trend in movement.

3.3 Iceberg freshwater flux uncertainty

The effect of errors in iceberg volume and velocity on our freshwater flux estimates is estimated using standard error propagation methods. Uncertainty in iceberg volume is derived from the calculation of iceberg surface area and the conversion of surface area to volume using Sulak et al.'s (2017) assumed relationship. Uncertainty in surface area is mainly due to mixed pixels from automatically identifying icebergs via thresholding. Automatic thresholding overestimates the surface area of each iceberg by ~12-18% (see supporting information), the average of which (15%) was applied as the overestimate for all icebergs, regardless of size.

The choice of threshold also adds uncertainty to our iceberg surface areas; comparison with five hand-delineated patches (~2.1 km^2 each) of high-resolution Planet Imagery (3 m pixels) from 15 June 2017 reveals that our choice of threshold overestimates surface area by ~4%, mostly through identifying false positives. For the conversion of iceberg surface area to volume, we use the uncertainty cited by Sulak et al. (2017) for their power law equation (6.0±2.59 and 1.3±0.04 for a and b, respectively in $V = aA^b$).

We apply a +11% uncertainty to our iceberg velocities, estimated as the average normalized percent difference between actual iceberg movement bearings and assumed linear bearings for 8 icebergs tracked via on-ice GPS units in Sermilik Fjord from summer 2017 (unpublished data; see supporting information). There is also uncertainty associated with using a linear regression to characterize iceberg volume change with distance down-fjord. Using the mean change in area-normalized iceberg volume with distance for all scenes to estimate freshwater fluxes results in a standard error of ~1.2 and 0.6 m^3 m^{-2} per km down-fjord for 2017 and 2018, respectively. In addition, the use of this relationship to estimate solid flux leaving the fjord introduces an uncertainty of ±8-13%, estimated by varying (according to standard error) the assumed slope and y-intercept of the linear fit between area-normalized volume and distance.

3.4 Estimating surface melt over Helheim, Fenris and Midgård glaciers

In order to compare our iceberg freshwater fluxes with other fluxes entering the fjord system, we estimate surface melt over the Helheim, Fenris and Midgård glacier catchments (Lewis, 2009), which we assume all exits each glacier at their respective grounding line. We use a positive degree day approach (Hock, 2003), with degree day factors for snow and ice of 3 and 9 mm °C d^{-1}, respectively (Fausto et al., 2009; Box, 2013; Enderlin and Hamilton, 2014) and a threshold snow melt temperature of 0 °C. Daily air temperature data for 2017-2018 were acquired from a Geological Survey of Denmark and Greenland PROMICE weather station located ~78 km SE of the HG terminus (Ahlstrøm et al., 2008; Figure 1a), and adjusted to glacier elevations using a Greenland-wide mean annual lapse rate of 6.8 °C km^{-1} (Fausto et al., 2009). Precipitation data were acquired from the Danish Meteorological Institute weather station in Tasiliaq, ~90 km SE of the glacier terminus (Cappelen, 2018; Figure 1a).

4 Results and Discussion

4.1 Iceberg velocity

Visually-tracked iceberg velocities reach up to 0.14±0.02 m s^{-1}, averaging 0.018±0.002 and 0.023±0.003 m s^{-1} in 2017 and 2018, respectively, with an overall down-fjord trend in movement (Figure S2; Table S2). Despite uncertainty, these velocities are in good agreement with down-fjord velocities measured using GPS-trackers in Sermilik Fjord in summer 2017 (following the methodology of Sutherland et al. (2014a)), which averaged 0.017 m s^{-1} (unpublished data). We find that down-fjord velocities are much higher than across-fjord velocities (Figure S2), and generally increase down-fjord on approaching the shelf break (e.g., Sutherland et al., 2014a). Due to the uncertainty associated with our velocity measurements, we use the mean iceberg velocities, 0.018 and 0.023 m s^{-1}, to estimate 2017 and 2018 freshwater fluxes, respectively.

4.2 Iceberg volume distributions

Total iceberg volume estimated for our study area ranges from 1.5 km^3 in June 2018 to 5.6 km^3 in late-July 2017 (Table S1), covering approximately 3.3 and 8.7% of the analyzed fjord surface, respectively. There is a greater number of icebergs in the fjord in 2017 compared to 2018, which is reflected in the lower overall volume of ice in the fjord in 2018 (Figure 2; Table S1). Although there is a greater number of smaller icebergs ($\leq 10^4$ m^3, 79-93% of all icebergs) during our study period, larger icebergs ($\geq 10^5$ m^3) dominate the fjord's iceberg volume, on average contributing 84% (Figure S3). This iceberg volume class distribution is similar to that seen in other Greenlandic fjords (e.g., Rink, Kangerlussuup and Ilulissat), as well as previously observed in Sermilik Fjord (e.g., Enderlin et al., 2016; Sulak et al., 2017). While variable through time, there is a strong and statistically significant (p-values from 1.0×10^{-10} to 0.006) observational decrease in area-normalized iceberg volume with distance down-fjord from HG throughout our study period (Figure 2; Figures S4-S5).

September has the highest volume of icebergs near the head of the fjord as well as the lowest volume of icebergs towards the fjord mouth in both 2017 and 2018, with volume dropping rapidly by mid-fjord (kms 61-64; Figure 2e). This distribution could result from a combination of generally increased iceberg calving rates in the months prior (e.g., Sulak et al., 2017) and warmer ocean temperatures in September (Straneo et al., 2010, Moon et al., 2017).

Due to the presence of a thick ice mélange, there is a lag between when icebergs calve from the glacier and when they enter the open-fjord (i.e., where we begin our measurements 37 km down-fjord from HG). This lag time varies annually in Sermilik Fjord, and was estimated as 16-39 days in September 2012 and over 120 days in August 2013 (Sutherland et al., 2014a). Based on average ice mélange speed in summer 2017-2018 (estimated here from tracking distinctive icebergs caught in the mélange), icebergs spend ~2 months travelling through the mélange before they reach the open-fjord. As such, higher iceberg calving fluxes from late-June to early-August (e.g., Sulak et al., 2017) would be reflected farther down-fjord in September, when we see higher iceberg volumes near the fjord head (Figure 2e). In addition, large, tabular calving events can accelerate the ice mélange and flush a considerable volume of ice into the open-fjord (e.g., Amundson et al., 2010; Murray et al., 2013). For example, a large calving event (~5 km^2 in surface area) occurred between 31st July and 2 August 2017 (Figure 1d), which accelerated the ice mélange from ~40 $m\ d^{-1}$ to just over 4 $km\ d^{-1}$, pushing a large volume of ice closer to the open-fjord. Additionally, a ~4 km^2 calving event occurred between the 14th and 17th of August 2017, which released more ice into the mélange and subsequently, open-fjord – reflected in our September 2017 estimates near the head of the fjord.

Warmer waters in Sermilik Fjord in September could cause a rapid decrease in iceberg volume consistent with our observations. On average, reported summer fjord water temperatures at various locations along Sermilik Fjord are cool just below the surface (approximately -1.5 to 0.5 ºC), increasing to 4 ºC at 450 m depth (Sutherland et al., 2014b, Moon et al., 2017). Average measurements taken in the fall show a warmer surface layer (0.5 to 1.5 ºC, < 100 m depth) and an extended warm layer between 100-250 m depth (Moon et al., 2017). In addition, water on the East Greenland Shelf (which eventually enters Sermilik Fjord) typically increases in temperature throughout the fall (Straneo et al., 2010). Warmer waters at middle depths in the water column accelerate iceberg melting, as larger icebergs have their keel depths here (e.g., Barker et al., 2004; Enderlin and Hamilton, 2014; Enderlin et al., 2016), while warmer surface waters accelerate the melting of smaller bergy bits and growlers. A combination of both warmer surface and mid-depth waters increases the rate of down-fjord iceberg volume loss compared to months with cooler water temperatures. Lower calving fluxes in September and October (Sulak et al., 2017), in combination with warmer fjord waters, likely result in the iceberg volume distribution observed in November 2017 (i.e., low volumes both near the head and mouth of the fjord; Figure 2f).

4.3 Freshwater flux from icebergs

Iceberg freshwater fluxes in Sermilik Fjord vary seasonally and with distance down-fjord from HG (Figure 3). Freshwater fluxes for 2018 are less than those estimated for 2017 in all months of our study, reflecting the decreased volume of ice in the fjord in 2018. Freshwater flux from icebergs peaks across August and September in both years, reaching approximately 3410±1975 and 1700±985 $m^3\ s^{-1}$ along the length of the fjord in 2017 and 2018, respectively (Figure 3a). Iceberg freshwater flux is relatively constant throughout June, July, October and November, ranging between 836±485 and 1270±735 $m^3\ s^{-1}$ (Figure 3a). Our estimated iceberg freshwater fluxes peak later in the summer than our modeled subglacial discharge from Helheim, Fenris and Midgård glaciers (Figure 3a), which peaks around 1400 and 787 $m^3\ s^{-1}$ on 26 July 2017 and 30 July 2018, respectively.

As with iceberg volume distributions, temporal variations in freshwater flux reflect seasonal ocean temperatures and calving fluxes, with warmer waters from September to November enhancing iceberg melt. Similar seasonal patterns have been seen in modeled iceberg melt rates and fluxes (e.g., Mugford and Dowdeswell, 2010; Moon et al., 2017), which show peak melt in early September, primarily due to warmer surface waters. Meltwater fluxes modelled by Moon et al. (2017) for a composite of different years reach ~1000±200 $m^3 s^{-1}$ in mid-September, roughly one-third and one-half of our peak flux estimates for late-summer 2017 and 2018, respectively. We would argue that our estimates are an improvement on the earlier results from Moon et al. (2017), which did not include freshwater flux from icebergs with long-axes > 30 m, a size class which contributes ~10-21% of our total iceberg volume. In addition, given the expected inter-annual variability in iceberg discharge, meteorological and oceanographic conditions, and the uncertainty inherent in both methods, we do not expect fluxes to be identical. The discrepancy between the reported values should be investigated in more detail.

Iceberg freshwater fluxes are highest near the head of the fjord (Figure 3b-d), where iceberg surface areas are largest, peaking at ~2800±1620 and 1320±765 $m^3 s^{-1}$ between 37 and 64 km down-fjord of HG for the two and one months prior to our mid-September 2017 and 2018 scenes, respectively (Figure 3c,d). As icebergs with larger surface areas typically have deeper drafts, a higher percentage of ice near the head of the fjord will be exposed to the warmest (up to 5.2 ºC; Jackson et al., 2014) waters located at depth in the water column, promoting more rapid submarine melting and increased freshwater flux. Icebergs with smaller drafts will sit in the cooler Polar Water layer, leading to comparatively lower meltwater fluxes. The spatial pattern in our iceberg freshwater fluxes is similar to that modeled by Moon et al. (2017), who showed a general decrease in freshwater flux with distance from HG, with a reduction of ~50% in the summer between 20-40 km and 80-100 km down-fjord. This is comparable to our July and August freshwater flux estimates, which decrease by ~48-60% between 37 – 64 km and 93 – 112 km down-fjord (Figure 3b,d).

Iceberg freshwater fluxes are also influenced by water velocities at the surface of the fjord and at depth, with fluxes increasing with velocity (Moon et al., 2017; Enderlin et al., 2018) in line with theoretical considerations of submarine melt (Jenkins, 2011). For example, a four-fold increase in deep-drafted iceberg melt rate was previously observed in Ilulissat Icefjord between late-March and early-April 2011, driven by an increase in turbulence-driven melt rate at depth due to an increase in water velocity triggered by a large calving event (Enderlin et al., 2018). Water velocities in Sermilik Fjord have been observed to vary significantly over a range of timescales, driven in part by velocity pulses from the shelf outside the fjord mouth (Jackson et al., 2014) and in part by subglacial melt driven fjord circulation (Cowton et al., 2015). Past observations in Sermilik Fjord show water velocities ranging from 0-0.8 $m s^{-1}$ (Jackson et al., 2014), fluctuating over timescales of hours to months and showing a slight reduction in velocity in June and July (as compared to September through May). Water velocities of surface down-fjord currents are also expected to increase with increasing subglacial runoff into the fjord system (Cowton et al., 2015), which peaks in late-July 2017 and 2018, with secondary peaks in early-September 2017 and early-August 2018 (Figure 3a). As such, high water velocities in late summer and fall could be contributing to our large freshwater fluxes estimated across August and September.

We also estimate a first-order approximation of the percentage of ice leaving the fjord as solid flux, using the difference in normalized ice volume between our first and last fjord sections (see supporting information). For the length of our study period, we estimate that on average between 9±8% (2018) and 14±13% (2017) of the calved input leaves the fjord as solid flux, indicating that most icebergs melt within the fjord thus delivering a significant amount of freshwater at depth to the fjord during the summer and fall. Our results therefore support previous conclusions on the critical importance of iceberg freshwater flux to the fjord budget (e.g., Enderlin et al., 2016; Moon et al., 2017).

The simple and easily transferable method for deriving iceberg freshwater fluxes in glacial fjords presented here confirms that iceberg melt contributes a significant volume of freshwater to the fjord, and that this freshwater enters the water column at depth along the full-fjord length. The volume of freshwater generated by the melting of icebergs in Sermilik Fjord exceeds the volume of subglacial discharge entering the fjord throughout the melt season and substantially so during spring, fall and winter. These findings demonstrate the importance of iceberg melt for water circulation, tidewater glacier submarine melt rate (e.g., Enderlin et al., 2016) and primary productivity (e.g., Smith et al., 2013; Meire et al., 2017) within fjord systems. In addition, these findings provide an independent estimate of iceberg melt, which could be used in future studies to differentiate between iceberg and terminus subglacial melt, a partitioning that is difficult to model or directly measure in glacial fjords.

5 Conclusions

We present a new methodology for estimating iceberg freshwater fluxes along glacial fjords, using freely available Sentinel-2 satellite imagery, which we use to estimate iceberg velocity and seasonal changes in iceberg volume with distance from Helheim Glacier during the summer and fall of 2017-2018. We estimate iceberg velocities up to 0.14 m s^{-1}, and find that in all months of our study iceberg volume decreases moving down-fjord away from the glacier terminus. We estimate maximum average 2-month total freshwater fluxes of ~1060±615, 1270±735, 1200±700, 3410±1975, and 1150±670 m^3 s^{-1} for the two months prior to the dates of our June, July, August, September and November scenes, respectively. Iceberg freshwater fluxes peak across August and September, reflecting warmer ocean temperatures and higher calving rates, and decrease with distance from the glacier terminus. We find that on average, only 9-14% of the ice calved into the fjord exits as solid flux, demonstrating that a significant volume of freshwater is released at depth along the length of the fjord. The volume of freshwater generated from iceberg melt exceeds the volume of subglacial discharge throughout the year with important implications for fjord-scale circulation, submarine melt rates, nutrient availability and primary productivity. Our method provides a valuable tool for monitoring iceberg freshwater fluxes and is a viable alternative to more complex methods for estimating flux from inaccessible fjords with no or limited field observations. We anticipate that our method and resulting fluxes could be used for constraining both fjord-scale and ice sheet wide ice-ocean models, which are critical for understanding future changes to the Greenland Ice Sheet and surrounding ocean basins.

Acknowledgments

Thank you to three anonymous reviewers and Donald Slater for their insightful recommendations. ANM is supported by a University of Edinburgh Principal's Career

Development PhD Scholarship. This work was also supported through a Postdoctoral and Early Career Researcher Exchange, funded by SAGES. DAS and PWN are partially supported by NSF Grant 1552232 and NERC grant NE/K015249/1, respectively. The imagery used in this study is freely available from ESA.

References

Ahlstrøm, A. P., Gravesen, P., Andersen, S. B., van As, D., Citterio, M., Fausto, R. S., Nielsen, S., Jepsen, H. F., Kristensen, S. S., Christensen, E. L., Stenseng, L., Forsberg, R., Hanson, S., Peterson, D., and the PROMICE Project Team (2008), A new programme for monitoring the mass loss of the Greenland ice sheet, Geol. Surv. Denmark Greenl. Bull., 15, 61-4.

Amundson, J. A., Fahnestock, M., Truffer, M., Brown, J., and M. P. Lüthi (2010), Ice mélange dynamics and implications for terminus stability, Jakobshavn Isbræ, Greenland, J. Geophys. Res., 115, F01005, doi: 10.1029/2009JF001405.

Barker, A., Sayed, M., and T. Carrieres (2004), Determination of Iceberg Draft, Mass and Cross-Sectional Areas, NRC Publications Archive (NPArC). In Proc. 14th Int. Offshore and Polar Engin. Conf., 899-904 (National Research Council Canada, Ottawa).

Box, J. E. (2013), Greenland Ice Sheet Mass Balance Reconstruction, Part II: Surface Mass Balance (1840-2010), J. Climate, 26, 6974-6989, doi: 10.1175/JCLI-D-12-00518.1.

Cappelen, J. (ed.) (2018), Greenland–DMI Historical Climate Data Collection 1784-2017, DMI Report 18-04, Copenhagen. Available online at: http://www.dmi.dk/laer-om/generelt/dmi-publikationer/.

Cowton, T., Slater, D., Sole, A., Goldberg, D., and P. Nienow (2015), Modeling the impact of glacial runoff on fjord circulation and submarine melt rate using a new subgrid-scale parameterization for glacial plumes, J. Geophys. Res. Oceans, 120, 796-812, doi: 10.1002/2014JC010324.

Enderlin, E. M., and G. S. Hamilton (2014), Estimates of iceberg submarine melting from high-resolution digital elevation models: application to Sermilik Fjord, East Greenland, J. Glaciol., 60(224), 1084-92, doi: 10.3189/2014JoG14J085.

Enderlin, E. M., Howat, I. M., Jeong, S., Noh, M-J., van Angelen, J. H., and M. R. van den Broeke (2014), An improved mass budget for the Greenland ice sheet, Geophys. Res. Lett., 41, 866-72, doi: 10.1002/2013GL059010.

Enderlin, E. M., Hamilton, G. S., Straneo, F., and D. A. Sutherland (2016), Iceberg meltwater fluxes dominate the freshwater budget in Greenland's iceberg-congested glacial fjords, Geophys. Res. Lett., 43, 11287-294, doi: 10.1002/2016GL070718.

Enderlin, E. M., Carrigan, C. J., Kochtitzky, W. H., Cuadros, A., Moon, T., and G. S. Hamilton (2018), Greenland iceberg melt variability from high-resolution satellite observations, Cryosphere, 12, 565-75, doi: 10.5194/tc-12-565-2018.

Fausto, R. S., Ahlstrøm, A. P., van As, D., Bøggild, C. E., and S. J. Johnsen (2009), A new present-day temperature parameterization for Greenland, J. Glaciol., 55, 95-105, doi: 10.3189/002214309788608985.

Gatti, A. and A. Bertolini (2015), Sentinel-2 Products Specification Document, Thales Alenia Space, Mérignac, France. Hock, R. (2003), Temperature index melt modelling in mountain areas, J. Hydro., 282, 104-115, doi: 10.1016/S0022-1694(03)00257-9.

Jackson, R. H., Straneo, F., and D. A. Sutherland (2014), Externally forced fluctuations in ocean temperature at Greenland glaciers in non-summer months, Nature Geosci., 7, 503-508, doi: 10.1038/NGEO2186.

Jenkins, A. (2011), Convenction-driven melting near the grounding lines of ice shelves and tidewater glaciers, J. Phys. Ocean, 41, 2279-2294, doi: 10.1175/JPO-D-11-03.1.

Kehrl, L. M., Joughin, I., Shearn, D. E., Floricioiu, D., and L. Krieger (2017), Seasonal and interannual variabilities in terminus position, glacier velocity, and surface elevation at Helheim and Kangerlussuaq Glaciers from 2008 to 2016, J. Geophys. Res. Earth Surf., 122, 1635-52, doi: 10.1002/2016JF004133.

Lewis, S. (2009), Hydrological Sub-basins of Greenland, Version 1. Boulder, Colorado USA. NSIDC: National Snow and Ice Data Center, doi: 10.5067/DT9T7DPD7HBI.

Luckman, A., Benn, D. I., Cottier, F., Bevan, S., Nilsen, F., and M. Inall (2015), Calving rates at tidewater glaciers vary strongly with ocean temperature, Nat. Commun., 6:8566, doi: 10.1038/ncomms9566.

Moon, T., Sutherland, D. A., Carroll, D., Felikson, D., Kehrl, L., and F. Straneo (2017), Subsurface iceberg melt key to Greenland fjord freshwater budget, Nature Geosci., 11, 49-54, doi: 10.1038/s41561-017-0018-z.

Mugford, R. I., and J. A. Dowdeswell (2010), Modeling iceberg-rafted sedimentation in high-latitude fjord environments, J. Geophys. Res., 115, F03024, doi: 10.1029/2009JF001564.

Murray, T., Selmes, N., James, T. D., Edwards, S., Martin, I., O'Farrell, T., Aspey, R., Rutt, I., Nettles, M., and T. Baugé (2013), Dynamics of glacier calving at the ungrounded margin of Helheim Glacier, southeast Greenland, J. Geophys. Res. Earth Surf., 120, 964-82, doi: 10.1002/2015JF003531.

O'Leary, M., and P. Christoffersen (2013), Calving on tidewater glaciers amplified by submarine frontal melting, Cryosphere, 7(1), 119-28, doi: 10.5194/tc-7-119-2013.

Rose, G. A. (2005), On distributional responses of North Atlantic fish to climate change, ICES J. of Marine Sci., 62(7), 1360-74, doi: 10.1016/j.icesjms.2005.05.007.

Smith Jr., K. L., Sherman, A. D., Shaw, T. J., and J. Sprintall (2013), Icebergs as Unique Lagrangian Ecosystems in Polar Seas, Annu. Rev. Mar. Sci., 5, 14.1-14.19, doi: 10.1146/annurev-marine-121211-172317.

Straneo, F., Hamilton, G. S., Sutherland, D. A., Stearns, L. A., Davidson, F., Hammill, M. O., Stenson, G. B., and A. Rosing-Asvid (2010), Rapid circulation of warm subtropical waters in a major glacial fjord in East Greenland, Nature Geosci., 3, 182-6, doi: 10.1038/ngeo764.

Straneo, F., Curry, R. G., Sutherland, D. A., Hamilton, G. S., Cenedese, C., Våge, K., and L. A. Stearns (2011), Impact of fjord dynamics and glacial runoff on the circulation near Helheim Glacier, Nature Geosci., 4, 322-7, doi: 10.1038/ngeo1109.

Sulak, D. J., Sutherland, D. A., Enderlin, E. M., Stearns, L. A., and G. S. Hamilton (2017), Iceberg properties and distributions in three Greenlandic fjords using satellite imagery, Ann. of Glaciol., 58(74), 92-106, doi: 10.1017/aog.2017.5.

Sutherland, D. A., Roth, G. E., Hamilton, G. S., Mernild, S. H., Stearns, L. A., and F. Straneo (2014a), Quantifying flow regimes in a Greenland glacial fjord using iceberg drifters, Geophys. Res. Lett., 41, 8411-20, doi: 10.1002/2014GL062256.

Sutherland, D. A., Straneo, F., and R. S. Pickart (2014b), Characteristics and dynamics of two major Greenland glacial fjords, J. Geophys. Res. Oceans, 119(6), 3767-91, doi: 10.1002/2013JC009786.

Figure Captions

Figure 1. (a) Sermilik Fjord from a Sentinel-2 image on 28 July 2017, including three large tidewater glaciers: Helheim (H), Fenris (F), and Midgård (M). White boxes are areas of the fjord included in the analysis, the green box indicates the extent of (b,c) and the orange box indicates the extent of (d); orange and pink triangles indicate locations of PROMICE MIT and DMI weather stations, respectively; (b) Automatically classified iceberg polygons (from 28 July 2017), highlighting pixels with TOA reflectance values ≥ 0.13; (c) Sample polygon tracking for velocity estimation of two distinct icebergs between 28-31 July, overlain on a Sentinel-2 image from 28 July 2017; (d) Terminus positions for Helheim, hand-digitized from Sentinel-2 and Landsat 8 band 8 imagery.

Figure 2. Area-normalized iceberg volume with distance down-fjord from HG for (a) all analysed Sentinel-2 scenes and for (b) June, (c) July, (d) August, (e) September and (f) November scenes. Solid and dashed black lines are regressions between area-normalized iceberg volume and distance down-fjord for 2017 and 2018 scenes, respectively. Coloured shading indicates 1σ around regressions. Separate figures for 2017 and 2018 scenes, including p-values for regressions, can be found in the supporting information (Figures S4 and S5).

Figure 3. (a) Average 2-month iceberg freshwater fluxes for the full length of Sermilik Fjord (bold lines spanning duration of flux, with dashed uncertainty boxes) and modelled subglacial discharge from Helheim, Fenris and Midgård glaciers through time; (b,d) average 2-month iceberg freshwater fluxes with distance from the glacier terminus for 2017 and 2018, respectively, where dashed vertical lines represent uncertainty in flux estimates. Note that for clarity, the dashed uncertainty lines for each month are slightly transposed from their respective points; (c) the same freshwater fluxes as in (b), but now including iceberg freshwater flux from 37-64 km down-fjord for the September scene (~2800 $m^3 s^{-1}$) which was not shown in (b) to allow for easier visualization of the other data.

Figure 1.

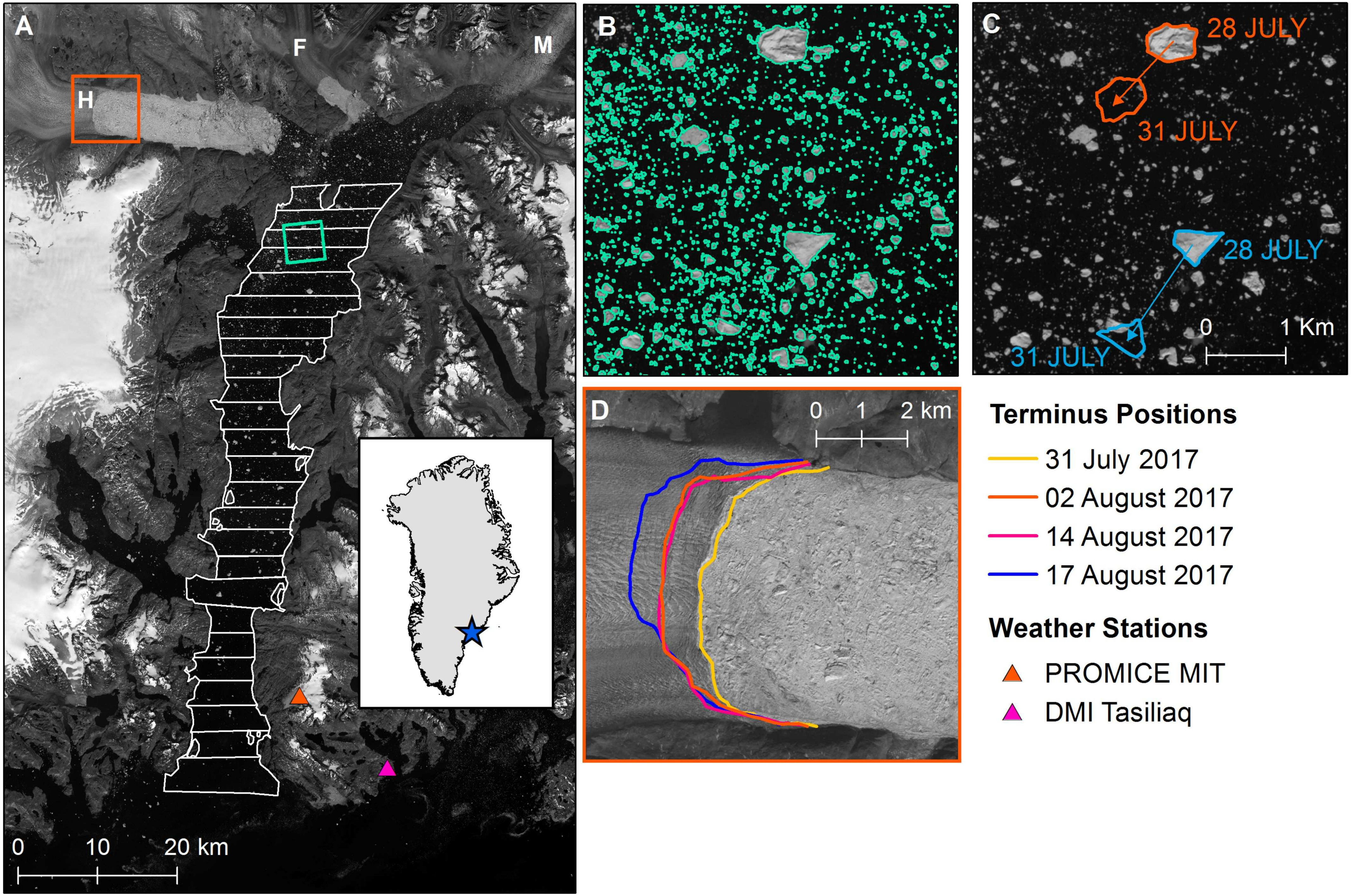
A
F
M
H
0
10
20 km
B
C
28 JULY
31 JULY
28 JULY
31 JULY
0
1 Km
D
0
1
2 km
Terminus Positions
31 July 2017
02 August 2017
14 August 2017
17 August 2017
Weather Stations
PROMICE MIT
DMI Tasiliaq

Figure 2.

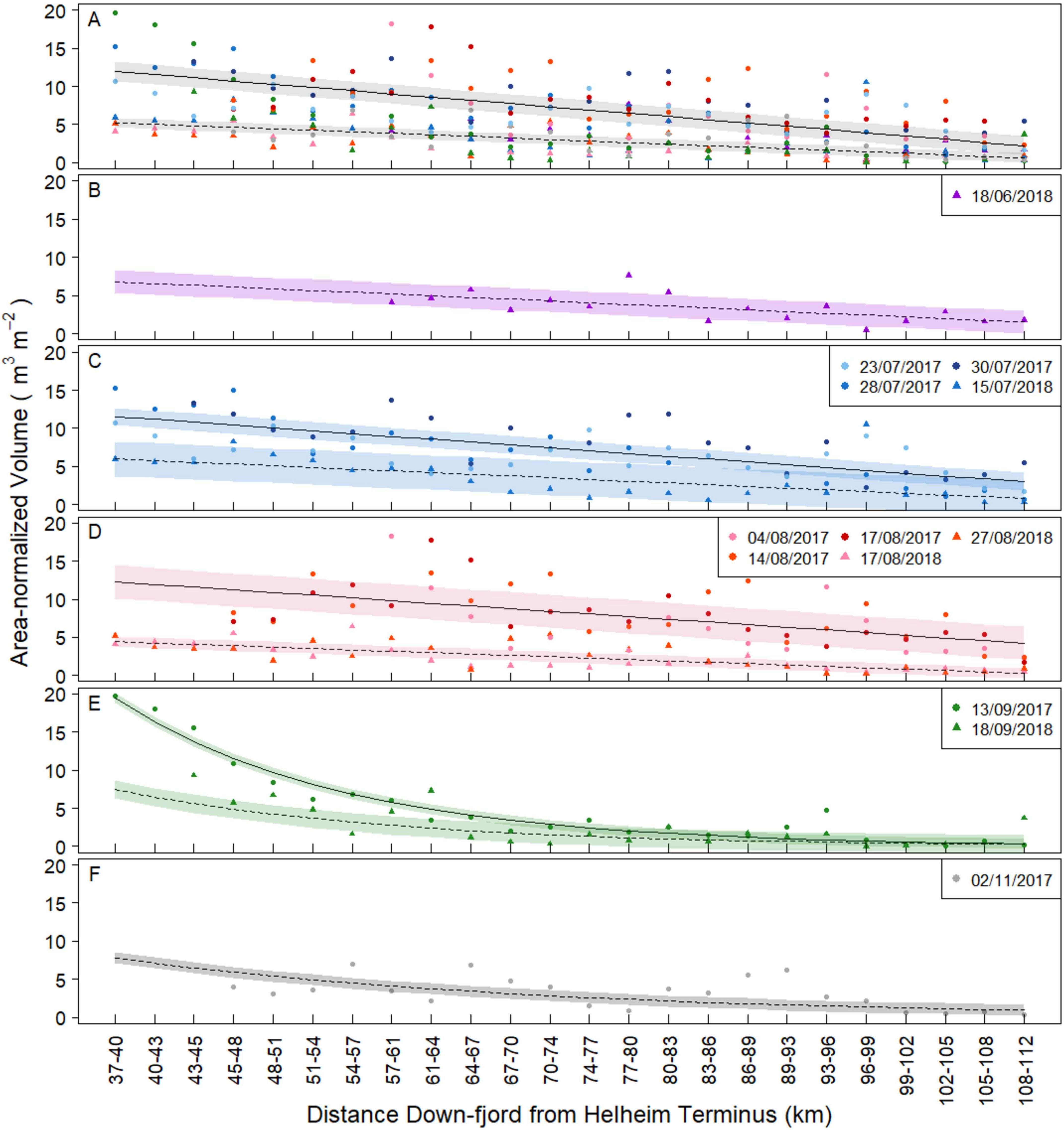
A
B
18/06/2018
C
23/07/2017
30/07/2017
28/07/2017
15/07/2018
D
04/08/2017
17/08/2017
27/08/2018
14/08/2017
17/08/2018
E
13/09/2017
18/09/2018
F
02/11/2017
Area-normalized Volume ($m^3 m^{-2}$)
Distance Down-fjord from Helheim Terminus (km)
37-40
40-43
43-45
45-48
48-51
51-54
54-57
57-61
61-64
64-67
67-70
70-74
74-77
77-80
80-83
83-86
86-89
89-93
93-96
96-99
99-102
102-105
105-108
108-112

Figure 3.

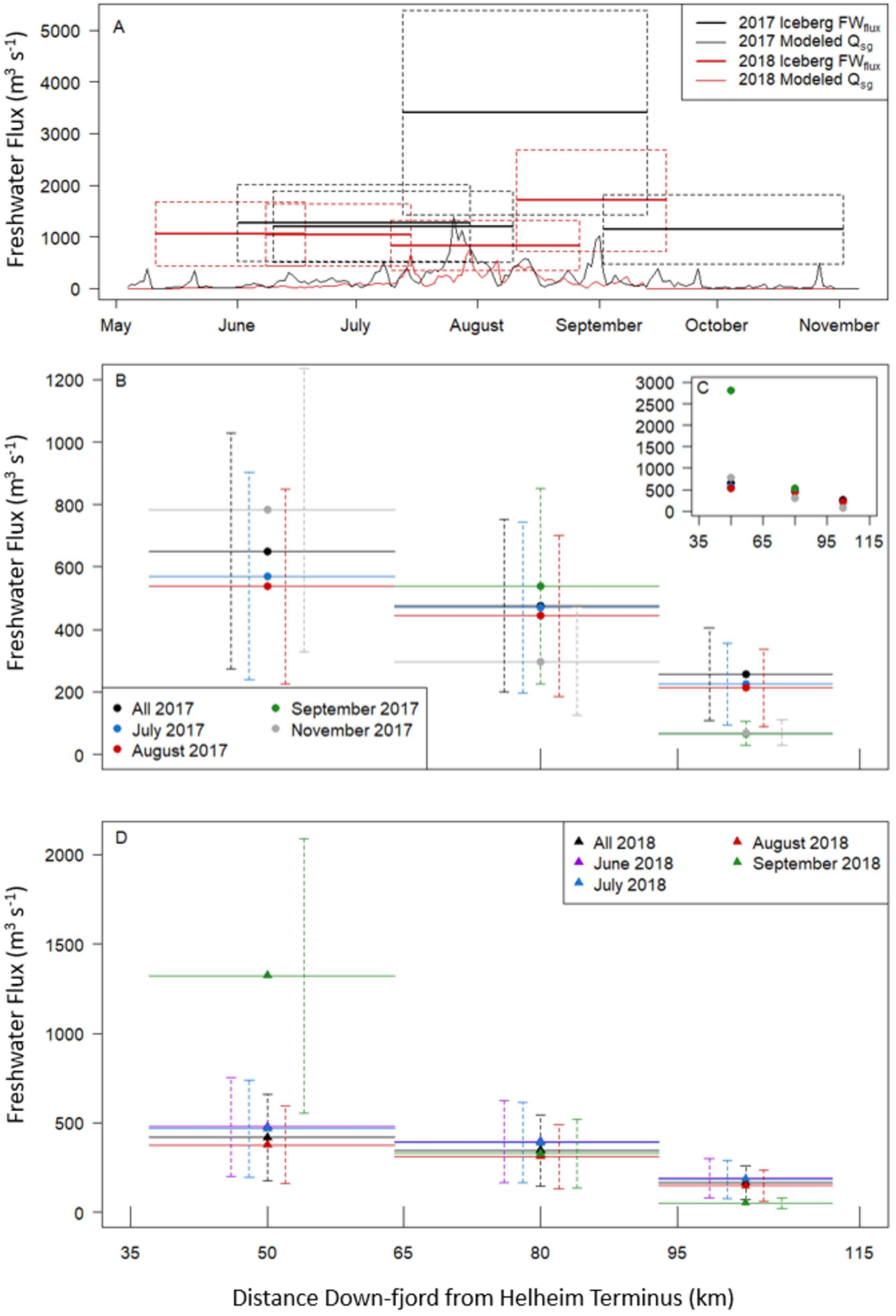

A
2017 Iceberg FW_flux
2017 Modeled Q_sg
2018 Iceberg FW_flux
2018 Modeled Q_sg
Freshwater Flux (m3 s-1)
0
1000
2000
3000
4000
5000
May
June
July
August
September
October
November
B
C
All 2017
July 2017
August 2017
September 2017
November 2017
0
200
400
600
800
1000
1200
0
500
1000
1500
2000
2500
3000
35
65
95
115
D
All 2018
June 2018
July 2018
August 2018
September 2018
0
500
1000
1500
2000
35
50
65
80
95
115
Distance Down-fjord from Helheim Terminus (km)